Low Power Consumption Multi-Channel RFoF System for Ka-Band Intra-Satellite Links

Yılmaz Uçar
Microwave Photonics GmbH
Oberhausen, Germany
yilmaz.ucar@microwave-photonics.com

Vitaly Rymanov
Microwave Photonics GmbH
Oberhausen, Germany
vitaly.rymanov@microwave-photonics.com

Sumer Makhlouf
Microwave Photonics GmbH
Oberhausen, Germany
sumer.makhlouf@microwave-photonics.com

Marcel Grzeslo
Microwave Photonics GmbH
Oberhausen, Germany
marcel.grzeslo@microwave-photonics.com

Riccardo Füllbrunn
Microwave Photonics GmbH
Oberhausen, Germany
riccardo.fuellbrunn@microwave-photonics.com

Andreas Stöhr
Microwave Photonics GmbH
Duisburg, Germany
andreas.stoehr@microwave-photonics.com

We developed multi-channel broadband radio frequency over fiber (RFoF) optical sub-assemblies (OSAs) for inter-equipment connectivity in Ka-band satellite communications. The RFoF transmitter OSA consists of 1.31 µm electro-absorptive modulated lasers (EMLs), while the receiver is fabricated using broadband 1.31 µm photodiodes with integrated transimpedance amplifiers (TIAs). The developed RFoF OSAs support four RF channels simultaneously and can be mounted directly onto the PCB via an RF interposer. Thanks to the EML, a low power consumption of 0.4 W per link is achieved. Due to the exploitation of the integrated TIAs, the link gain is beyond 0 dB over the entire uplink Ka-band between 27-32 GHz for all four channels. Noise and non-linearity experimental characterization reveal a noise figure approximately 43 dB and a phase noise at 30 GHz of - 120 dBc/Hz at 1 MHz offset. The saturated output power and SFDR are around -7 dBm and 84 dBc, respectively.

Keywords—photonic integrated circuit, radio over fiber, microwave photonics, intra-satellite link

I. Introduction

Photonic technologies are considered as key enablers for space [1-4] and numerous other applications. Especially, Radio frequency over fiber (RFoF) systems replacing conventional copper-based cabling attracted significant attention due to the inherent low weight, low loss and compact structure of optical fibers. A particularly promising application of RFoF systems lies in providing inter-equipment connectivity in satellite communications, e.g. by interconnecting the processing unit with the remoted antennas. Conventionally, inter-equipment connectivity in satellites has relied on copper-based cabling, which is both lossy and bulky. The significance of minimizing loss, weight and footprint of these links becomes paramount when the number of intra-satellite links is considered. Consequently, there is a compelling need to transition from the conventional approach to advanced RFoF systems. Inherent KPIs for such RFoF systems include broadband operation, high linearity, and hermetic packaging. Current RFoF systems can meet these requirements, however, they are lacking in certain specifications that are significant for space applications, such as low power consumption and solderless integration.

In this work, we present the development and characterization of novel low power consumption, small size and low weight RFoF optical sub-assemblies (OSAs). The OSAs consist of broadband 1.31 µm electro-absorptive modulated lasers (EMLs), 1.31 µm photodiodes and transimpedance amplifiers (TIAs) and support concurrent operation for four Ka-band uplinks between 27-32 GHz. To support solderless integration, an innovative packaging and RF interposer technology are exploited. The fabricated RFoF OSAs are experimentally characterized in terms of link gain, saturated output power, noise figure (NF), phase noise and spurious-free dynamic range (SFDR).

The authors acknowledge financial support from the European Commission in the framework of the TERAOPTICS project (grant no. 956857), and PATTERN project (grant no. 101070506).

II. RFoF System Development

The RFoF system consists of a transmitter module and a receiver module, each connected by fiber optic multi-port terminals featuring multiple fibers. Interfacing of the modules is provided by interposers, evaluation boards and mechanical carriers. The transmitter module is based on four 1.31 µm uncooled electro-absorptive modulated laser chip-on-carriers. EMLs merge optical carrier generation and RF modulation by employing a distributed feedback (DFB) laser and an electro-absorption modulator (EAM). Thereby, low driving requirements, compact size and high fabrication capability are achieved [5]. Due to the uncooled operation of the exploited EMLs, the use of a thermo-electric cooler in the transmitter is eliminated resulting in a drastic reduction of the power consumption of the system. In the receiver module, four independent photoreceivers are implemented. Each photoreceiver contains four high-frequency 1.31 µm arrayed PIN photodiodes integrated with gain-controllable TIAs. The TIAs are deployed to compensate the losses introduced by the RFoF link, i.e. the slope efficiency of the EAM and responsivity of the photodiodes. The block diagram of the RFoF system is depicted in Fig. 1.

In the packaging process of the modules, the EMLs and photoreceivers are assembled into a hermetically sealed OSA. The OSA contains optical beam steering to guide the light

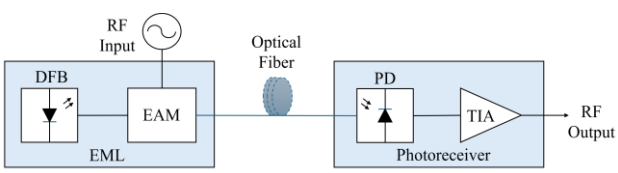

Fig. 1. Block diagram of the RFoF link. The RFoF transmitter OSA consists of a 1.31 µm DFB laser integrated with an EAM. The receiver is realized using a 1.31 µm photodiode and a broadband TIA.

between chip facets and mechanical transfer (MT) ferrules of the modules by using prisms and lenses.

To provide the DC and RF connectivity for the multi-channel transmitter and receiver modules, the packaging features land grid arrays (LGAs) which cannot be directly mounted on the evaluation board. Therefore, an innovative interposer technology is exploited enabling a solderless connection between evaluation board and the modules. This is crucial in space applications since soldering is prone to malfunctioning in harsh environments. The assembly of each module is depicted in Fig. 2 while the entire multi-channel RFoF system is shown in Fig. 3.

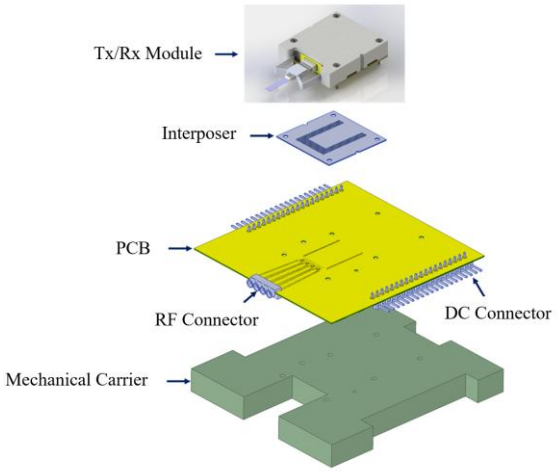

Fig. 2. Assembly of an RFoF OSA. The Tx/Rx modules are mounted on a PCB via an interposer. Mechanical stability is provided by the mechanical carrier.

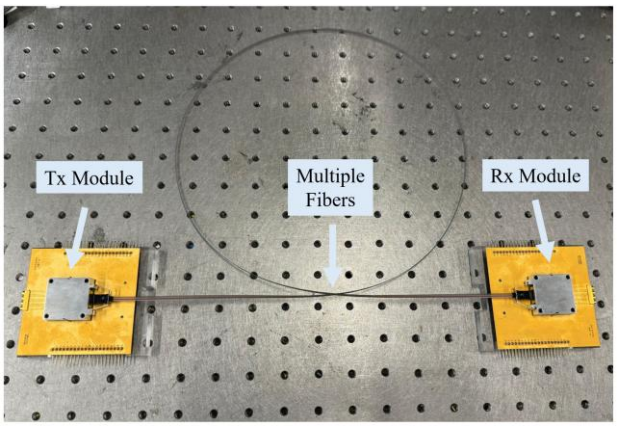

Fig. 3. Photo of the fabricated four-channel RFoF transmitter and receiver OSAs mounted on PCBs and interconnected by a multi-terminal fiber.

III. RFoF System Characterization

In this section, the characterization of the developed RFoF system is presented, and general key parameters of the system are provided. In addition to link gain measurements, a detailed analysis of the system in terms of noise and non-linearity is conducted.

A. *Link Gain*

To estimate the loss of the entire RFoF link, link gain measurements are conducted. The link gain itself is defined as the ratio between RF output power and RF input power of the link at a specific frequency. Here, it is measured using a vector network analyzer (VNA, *Rohde&Schwarz*, ZNA67) within the frequency range of 27-32 GHz at -10 dBm RF input power and the results are depicted in Fig. 4. The results demonstrate that the link gains of all channels are higher than 0 dB over the whole frequency range which indicates that the introduced losses are compensated by the TIAs. It is evident that the link gain of each channel slightly varies from the others. This is due to the fact that the inherent characteristics of the individual components within the system, namely the responsivity of the photodiodes and the optical output power of the lasers, differ for each channel. The link gain variation between the channels can be optimized by adjusting the gain of each TIA.

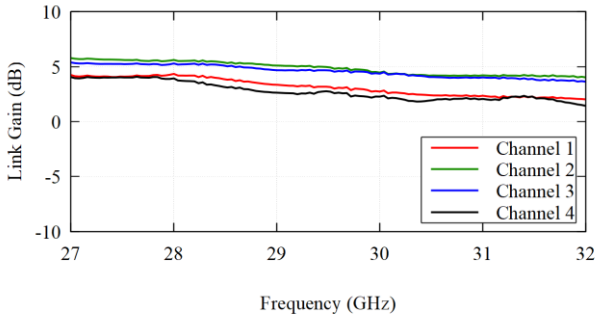

Fig. 4. RFoF link gain for all four-channels between 27-32 GHz at -10 dBm RF input power for each channel.

B. *Saturated Output Power*

Since a linear response of the RFoF link is an important figure of merit, it is crucial to analyze the power limitations which can cause non-linearity in the system. Thus, saturated output power measurements are performed. As the system is designed for an input power of -10 dBm, characterization was carried out in an input power range from -30 dBm to +10 dBm at a frequency of 30 GHz using the VNA. The results are depicted in Fig. 5 and show a linear response until approximately -8 dBm RF input power. For higher input powers, the system starts to saturate, reaching a maximum RF output power of approximately -7 dBm. Notably, the system maintains functionality up to an input power of +10 dBm demonstrating that the system can maintain resilient operation in the presence of interference.

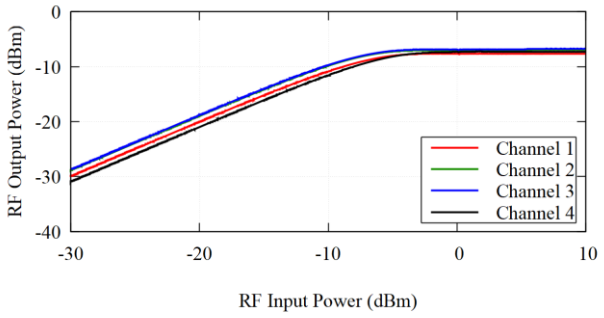

Fig. 5. Saturated output power at 30 GHz for all four channels versus RF input power between -30 dBm to +10 dBm.

C. Noise Figure

Noise characterization of a system is a crucial figure of merit, and the most common noise characterization technique of such system is the noise figure analysis. Thus, noise figure measurements are performed in frequency range of 27-32 GHz at -10 dBm RF input power using the VNA. The VNA utilizes the cold source technique, which combines the output noise power measurement of the device under test (DUT) with an available gain measurement to calculate the noise figure of the DUT. The results are depicted in Fig. 6 demonstrating around 43 dB noise figure over the frequency range. The main contributors of the NF are relative intensity noise of the laser, shot noise of the photodiode and thermal noise of the system.

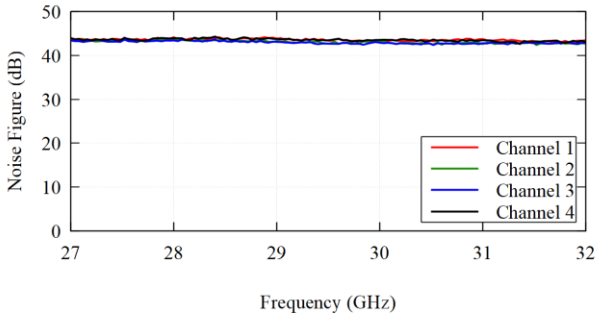

Fig. 6. Noise figure of all four links over frequency for the 27-32 GHz Ka-uplink band at -10 dBm RF input power.

D. Phase Noise

The aim of the measurement is to analyze the phase noise constrain of the system over the signal to be transmitted through the link. The phase noise of the link is characterized using a dedicated phase noise analyzer (*Rohde & Schwarz*, FSWP50) which its ultra-low phase noise internal source is configured to generate an RF power of -10 dBm at 18 GHz. The results are depicted in Fig. 7 after scaling it to 30 GHz.

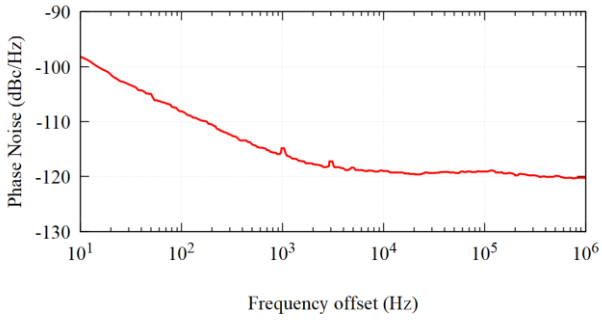

Fig. 7. Phase noise of a single-channel RFoF link at -10 dBm RF input power scaled to 30 GHz RF frequency.

The measurement results demonstrate that the RFoF link has a phase noise level around -120 dBc/Hz at 1 MHz offset frequency. As can be seen from Fig. 7, at high offset frequencies the phase noise exhibits a white noise characteristic. The broadband behavior of the link's phase noise can be expressed in relation to the noise figure by using (1), where N_{TH} is thermal noise floor and P_{in} is the RF input power [6]. When the obtained noise figure results from the previous section are included in (1), it can be concluded that noise measurement results are in a good agreement.

$$L(f) = N_{TH}+NF-P_{in} \quad (1)$$

E. Spurious-free Dynamic Range

Further non-linearity analysis of the system is carried out by two-tone SFDR measurements. For this purpose, the RF input signals are adjusted to be 10 MHz apart, i.e. 30 GHz and 30.010 GHz, and provide -10 dBm power after a power combiner. The input power is reduced systematically while the power level of the fundamental tone and third order harmonic are analyzed using an electrical spectrum analyzer. The results are depicted in Fig. 8.

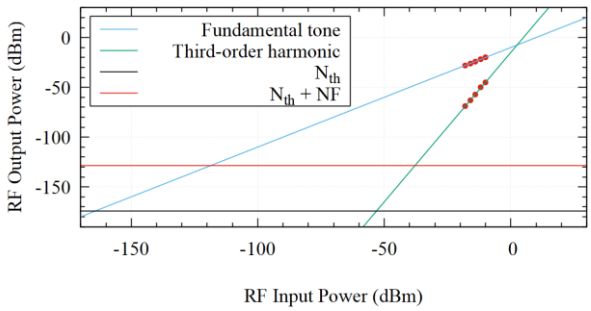

Fig. 8. Two-tone SFDR measurement of a single RFoF link for 30 GHz and 30.010 GHz RF input signals .

The measured data points show for the fundamental tone a power reduction slope of 1 while for the third order harmonic a slope of 3 is obtained which is in agreement with the theory. Based on that, the SFDR is calculated where the third order harmonic is suppressed to the noise floor resulting in SFDR of around 84 dBc.

F. General Key Parameters

As previously stated in the introduction, it is crucial to minimize the size and the weight of the interconnections in a satellite to free space and reduce the launching cost. In our system, this is provided by exploiting optical fiber and multi-channel operation. As can be seen from Table 1, the total weight of the whole link, including the transmitter module, the receiver module and the 1 m fiber, is less than 50 g, mainly determined by the weight of the modules. Even with a transmission range of 1 m, the weight of the four-channel system is equivalent to half that of a standard 1 m single channel RF cable. The weight benefit of such a system becomes even more apparent when the length of the intra-satellite link is increased. Power consumption is another key parameter, given the limited availability of power sources in space applications. The implementation of the uncooled EMLs enables a substantial reduction in the power consumption of the developed RFoF system. The system exhibits a power consumption of less than 0.4 W per channel which is ten times lower compared to typical RFoF systems. The power consumption, weight and size features of the RFoF link are shown in Table 1.

TABLE I. GENERAL KEY PARAMETERS

Key Parameters	
Power consumption per channel	< 0.4 W
Weight of the whole link	< 50 g
Footprint per module	30 cm^2

IV. CONCLUSION

We demonstrated RFoF OSAs for replacing conventional copper-based cabling in satellite communications. The developed OSAs support four RF Ka-band uplink channels simultaneously and can be mounted solderless on satellite's main board thanks to the RF interposer technology exploited. Low power consumption of less than 0.4 W per RF channel with a positive link gain >0 dB across the entire uplink Ka-band 27-32 GHz is achieved by exploiting uncooled EMLs and TIAs. Furthermore, the RFoF OSAs provide a low phase noise at 30 GHz of -120 dBc/Hz at 1 MHz offset as well as s high saturation RF output power of -7 dBm and a high SFDR of 84 dBc. The OSAs even support entire ITU approved Ka-band satellite networks in the 17.3-31 GHz frequency range.

REFERENCES

[1] J. Anzalchi, P. Inigo and B. Roy, "Application of photonics in next generation telecommunication satellites payloads," International Conference on Space Optics (ICSO 2014), Vol. 10563, pp. 1063-1071, November 2017.

[2] L. Rodio, V. Schena, M. Grande, G. Calò and A. D'Orazio, "Microwave-photonic technologies for satellite telecommunication payloads: a focus on photonic RF frequency conversion," IEEE 8th International Workshop on Metrology for AeroSpace (MetroAeroSpace), Naples, Italy, 2021, pp. 154-158.

[3] P. Inigo et al., "Review of terabit/s satellite, the next generation of HTS systems," 7th Advanced Satellite Multimedia Systems Conference and the 13th Signal Processing for Space Communications Workshop (ASMS/SPSC), Livorno, Italy, 2014, pp. 318-322.

[4] G. Charalampous and S. Iezekiel, "Microwave photonic frequency generation and conversion unit design for Ka-band satellite payloads," Proc. SPIE 11852, International Conference on Space Optics (ICSO 2020), Vol. 11852, pp. 1745-1753, June 2021.

[5] B. Schrenk, "Electroabsorption-modulated laser as optical transmitter and receiver: status and opportunities," IET Optoelectron., 14: 374-385, 2020

[6] E. Rubiola, Phase Noise and Frequency Stability in Oscillators. Cambridge, Cambridge University Press, 2008.